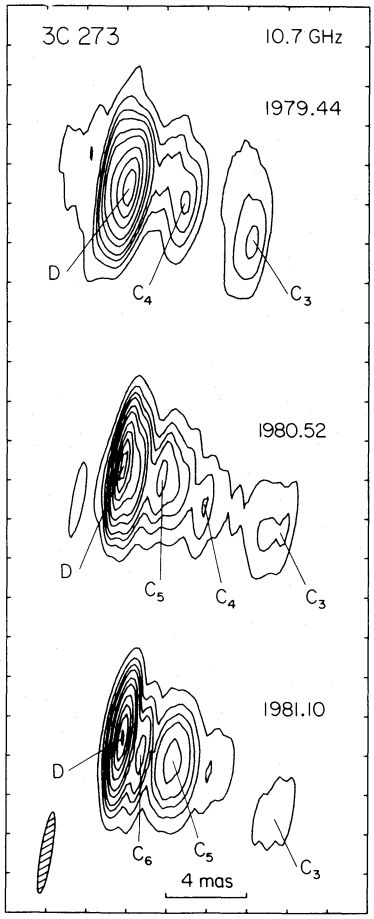

FIG. 3

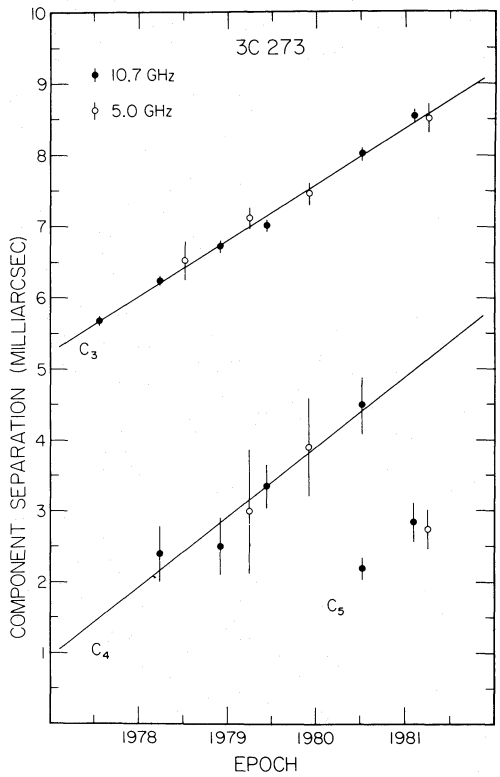

FIG. 4

FIG. 3.—Hybrid maps of the compact radio structure in 3C 273 at 10.7 GHz, made with a beam size of 4.2 × 0.55 mas in P.A. −10°. Contours are drawn at 0.2, 0.4, 0.7, 1.0, 1.5, 2, 3, 4, 6, 8, . . . , 18 Jy per beam area. There are no negative areas below −0.2Jy per beam area. Other details as in Fig. 1.

FIG. 4.—Separation of components in the 3C 273 jet from the core at 5.0 and 10.7 GHz, as a function of observing epoch. Measurements of C_3 from P81 are also shown. The straight lines represent linear least squares fits to the observed points, shown with $\pm 1\sigma$ error bars estimated from the map measurements.

until 1981.26. Following P81, we aligned the maps as described in § III above, and measured the radial distances of the various components from the core. The results are plotted on the time sequence shown in Figure 4. They are most extensive for knot C_3, which continues to show a steady proper motion, with no evidence of acceleration. Furthermore, its position is independent of frequency (between 5.0 and 10.7 GHz), so there are no significant spectral gradients across it. (We believe that there is no significant frequency dependence in the position of the reference point; see § V*c*.)

Table 2 gives the results of a linear least squares fit to the motion of components C_3 and C_4, both of which are superluminal relative to the core D. When we discuss superluminal motion, we assume that the core D is stationary, from arguments in P81 and U83, and by analogy with 3C 345, for which an absolute measurement has been made by Bartel *et al.* (1984). There is considerable scatter in the measurements of C_4, due to blending with adjacent features, but the speed is consistent with that of C_3. Only three measurements of the position of C_5 are available, but they are again consistent with superluminal motion at $v/c \approx 6\ h^{-1}$. The uncertainty is large because C_5 is resolved, and appears to change shape, so it has no single well-defined velocity.

b) Evolution of Component Brightness

The maps in Figures 1–3 show evolution of the component flux densities, as well as proper motion. To study these changes quantitatively, we estimated the flux densities of each com-

TABLE 2

SUPERLUMINAL MOTION IN THE 3C 273 JET

Component	C_3	C_4
Proper motion[a] (mas yr^{-1})	0.79 ± 0.03	0.99 ± 0.24
Apparent transverse velocity[b]	(5.5 ± 0.2) $h^{-1}c$	(6.9 ± 1.7) $h^{-1}c$
Epoch of zero separation[a] (yr)	1970.3 ± 0.2	1976.0 ± 0.6

[a] Assuming constant velocity.

[b] Relative to the core D (Hubble constant $H_0 = 100h$ km s^{-1} Mpc^{-1}).